Sphk1 regulates HMGB1 via HDAC4 and mediates epithelial pyroptosis in allergic rhinitis

Wei Huang , MM[1], Xi Chen , MM[1], Zizhen Liu , MM, Changwu Li , MD, Xin Wei , MD, Jiabin Zhan , MD, Quan Qiu , MM and Jing Zheng , MD*

ABSTRACT

Background: Allergic rhinitis (AR) is a global health issue affecting millions of individuals worldwide. Pyroptosis has emerged as a major player in the development of AR, and targeting its inhibition with specific drugs holds promise for AR treatment. However, a comprehensive understanding of the precise mechanisms underlying pyroptosis in AR remains to be explored, warranting further investigation.

Objective: This study aims to elucidate the roles of HMGB1, Sphk1, and HDAC4 in regulating human nasal epithelial cell (hNEC) pyroptosis and AR.

Methods: An *in vitro* AR cell culture model and *an in vivo* AR mouse model were established. Western blot, ELISA, histological staining, and flow cytometry were utilized to confirm the gene and protein expression. The interactions among Sphk1, HDAC4, and HMGB1 were validated through ChIP, Co-IP, and Dual-luciferase assay.

Results and conclusion: We identified that the expression levels of Sphk1, HMGB1, and inflammasome components, including IL-18, and IL-1β were elevated in AR patients and mouse models. Knockdown of Sphk1 inhibited hNEC pyroptosis induced by dust mite allergen. Overexpression of HDAC4 suppressed HMGB1-mediated pyroptosis in hNECs. In addition, HDAC4 was found to mediate the transcriptional regulation of HMGB1 via MEF2C, a transcription factor. Additionally, Sphk1 was shown to interact with CaMKII-δ, promoting the phosphorylation of HDAC4 and inhibiting its cytoplasmic translocation. Knockdown of HDAC4 reversed the effect of Sphk1 knockdown on pyroptosis. These discoveries offer a glimpse into the molecular mechanisms underlying AR and suggest potential therapeutic targets for the treatment of this condition.

Keywords: Sphingosine kinase 1, HMGB1, HDAC4, Pyroptosis, Rhinitis, Allergic

Department of Otorhinolaryngology Head and Neck Surgery, Hainan General Hospital, Hainan Affiliated Hospital of Hainan Medical University, Haikou 570311, Hainan Province, PR China
*Corresponding author. Department of Otorhinolaryngology Head and Neck Surgery, Hainan General Hospital, Hainan Affiliated Hospital of Hainan Medical University, No.19, Xiuhua Road, Xiuying District, Haikou 570311, Hainan Province, PR China. E-mail: serena_zheng@163.com
[1] Wei Huang and Xi Chen are the co-first authors.
Full list of author information is available at the end of the article

INTRODUCTION

Allergic rhinitis (AR) is an atopic disorder characterized by nasal congestion, clear rhinorrhea, sneezing, postnasal drip, and nasal itching.[1] It poses a significant worldwide health issue, impacting around 400 million individuals across the globe.[2] Previous studies have classified AR into 2 phenotypes: rhinitis alone, which accounts for 70–80% of AR patients, and rhinitis with multimorbidity such as asthma, which accounts for 20–30%.[3] Over the years, the prevalence of AR has risen, largely attributed to the escalation of urbanization and the presence of environmental pollutants, which are considered major contributing factors to this condition.[2] Although AR is non-fatal and often overlooked, AR patients endure a considerable amount of physical discomfort and psychological stress, significantly impacting their overall quality of life.[4] Understanding the underlying pathophysiology of AR is essential for the advancement of innovative therapies for this disease.

The inflammasome plays a central role in initiating and controlling the innate immune response in AR.[1] It acts as a critical signaling platform, responsible for processing various pathogenic and cellular products linked to stress and injury.[1] NOD-like receptor family pyrin domain-containing protein 3 (NLRP3) inflammasome is a cytoplasmic protein complex consisting of NLRP3, apoptosis-associated speck-like protein containing a caspase recruitment domain (ASC), and pro-caspase-1.[5] When the NLRP3 inflammasome is activated, pro-caspase-1 is cleaved into its active form, caspase-1, which then induces the release of interleukin-1 beta (IL-1β) and IL-18, triggering cell pyroptosis and cell death.[6] Recent studies have documented pyroptosis, a form of programmed cell death linked to the activation of inflammasomes and inflammatory caspases, which in turn aggravates AR.[1] For example, Wang et al discovered that Xiaoqinglong decoction alleviated AR by suppressing NLRP3-mediated pyroptosis in BALB/c mice.[7] Additionally, another group reported that the activation of the NLRP3 inflammasome induced an inflammatory reaction in AR through pyroptosis of macrophage.[8]

High mobility group box 1 (HMGB1), a pro-inflammatory factor that has the potential to become an effective innovative therapeutic target for chronic upper respiratory tract inflammation and mucosal inflammatory diseases, can enhance the expression of NLRP3 in epithelial cells.[9] Under normal conditions, the HMGB1 protein is localized in the nucleus of eukaryotic cells, where it tightly binds to DNA and regulates nucleosome stability, DNA recombination, replication, repair, and transcription.[10] However, upon its extracellular release, it functions as a stimulator of innate immunity and a highly influential inflammatory agent.[10] Studies have confirmed a significant upregulation of the HMGB1 protein expression in airway epithelial cells of asthmatic patients.[11] Increased expression of HMGB1 has also been found in AR patients,[12] and high levels of HMGB1 in the nasal cavity are closely correlated with the severity of symptoms,[13] suggesting HMGB1 is a promising target for AR treatment. Nevertheless, the mechanism underlying HMGB1-mediated NLRP3 inflammasome-related pyroptosis and AR remains to be elucidated to provide better insight.

During the translocation and release of HMGB1, protein acetylation modification plays an important role.[14] Upon acetylation modification, the spatial conformation of HMGB1 changes, resulting in decreased affinity for DNA, translocation from the nucleus to the cytoplasm, and subsequent active secretion into the extracellular space.[14] A recently published study on septic liver injury has shown that inhibiting sphingosine kinase 1 (Sphk1), can significantly reduce HMGB1 acetylation and intracellular translocation in sepsis-related liver injury.[15] Sphk1 catalyzes the production of sphingosine-1-phosphate (S1P) and plays an important role in inflammatory responses.[16] Moreover, studies have indicated that Sphk1 is involved in the regulation of cell pyroptosis.[17] Although the role of Sphk1 in AR has not been reported in the literature, S1P produced by Sphk1 plays a critical role in AR, specifically rhinitis alone phenotype, and targeting S1P and sphingosine lyase can alleviate AR.[18] Therefore, we speculated that Sphk1 may participate in regulating AR via mediating HMGB1.

The study also suggests that Sphk1 directly interacted with calcium/calmodulin-dependent protein kinase II-δ (CaMKII-δ) to mediate histone deacetylase 4 (HDAC4) phosphorylation in Kupffer cells.[15] Under normal conditions, HDAC4 is

phosphorylated and sequestered in the cytoplasm, and dephosphorylation of HDAC4 leads to its nuclear translocation.[19] Inhibition of Sphk1 reduced the phosphorylation of CaMKII-δ, resulting in a decrease in HDAC4 phosphorylation and inhibition of HDAC4 translocation from the cytoplasm to the nucleus.[15] HDAC4 was shown to be involved in modulating AR. The activation of sirtuin 1/nuclear factor kappa-light-chain-enhancer of activated B cells (SIRT1/NF-κB) signaling through HDAC4 depletion has shown promising results in alleviating the IL-13-induced inflammatory response and excessive mucus production in nasal epithelial cells.[20] Furthermore, our preliminary data showed that the transcription factor myocyte-specific enhancer factor 2C (MEF2C), known to interact with HDAC4, was expected to bind to specific regions of the HMGB1 promoter regions, including BS1 and BS2. This suggests that HDAC4 may potentially regulate HMGB1 via MEF2C.

Thus, we hypothesized that Sphk1 interacts with CaMKII-δ, promoting the phosphorylation of HDAC4 and inhibiting the cytoplasmic translocation of HDAC4 in human nasal epithelial cells (hNECs). This leads to a decrease in nuclear HDAC4, which induces the expression and release of HMGB1 via MEF2C and contributes to pyroptosis-mediated inflammation and AR. This study aims to explore the role of Sphk1 in regulating hNEC pyroptosis and AR and the underlying mechanisms. First, the expression levels of Sphk1 were examined in human samples and *in vivo* AR mouse models. Next, hNECs were used to create an *in vitro* model to explore the regulatory roles of Sphk1, HMGB1, and HDAC4. Ultimately, the *in vitro* findings were validated in *in vivo* AR mouse models.

MATERIALS AND METHODS

Clinical sample collection

Before enrollment, written informed content was received from each patient. The study was proved by our hospital. The ethics committee approval number is Med-Eth-Re[2022]562. Nasal lavage fluid (NLF) and nasal mucosa tissues were collected from 40 AR patients and 10 healthy controls, respectively.

Cell culture

Using interdental brushes, primary hNECs were obtained from the middle part of the inferior turbinate of patients with dust mite-induced AR based on a previously published protocol.[21] In brief, the patients underwent paired nasal brushing while under general anesthesia for a clinically indicated procedure. The participants were positioned supine with their heads in the "sniffing" position to maintain an open airway. Before brushing the inferior nasal turbinate, we applied 0.9% saline drops to the nasal passage and removed visible mucus with gauze. Each participant then had 1 inferior nasal turbinate brushed with the Olympus brush and the opposite inferior nasal turbinate brushed with the Endoscan brush. The brushing procedure was standardized, with the same operator performing all procedures and conducting three rotations with each brush in each nostril. The collected hNECs were carefully removed from the brush and gently vortexed to dissociate them. They were then passed through a cell strainer (Sigma-Aldrich, St. Louis, MO, USA, CLS431750) to ensure a uniform cell suspension. Afterward, the cells were pelleted and reconstituted in 1 mL of media. The cells were expanded through 2 passages using serum-free bronchial epithelial cell basal medium (BEBM, Lonza Walkersville, Inc.; Walkersville, MD, USA). The medium was supplemented with 1% v/v bovine pituitary extract, 0.5 μg/mL hydrocortisone, 5 μg/mL insulin, 50 μg/mL gentamicin, 0.1 ng/mL retinoic acid, 50 μg/mL amphotericin B, 6.5 μg/mL triiodothyronine, 10 μg/mL transferrin, 0.5 ng/mL epidermal growth factor (Lonza Walkersville, Inc.), 0.5 μg/mL epinephrine, 100 μg/mL streptomycin, and 100 U/mL penicillin (Sigma-Aldrich). The cells were incubated in a humidified atmosphere with 5% CO_2 and 95% air at 37 °C. Cells from the second passage were frozen in liquid nitrogen and stored for use in subsequent passage 2–3 experiments. Besides, HEK293T cells were obtained from ATCC (American Type Culture Collection, Manassas, VA, USA), and were grown in Dulbecco's Modified Eagle Medium (DMEM) containing 10% FBS (fetal bovine serum, Gibco, Grand Island, NY, USA).

Establishment of ovalbumin (OVA)-induced AR mouse model and *in vitro* AR cell model

This study received ethical approval from our hospital for all animal experiments conducted. Balb/c mice aged between 7 and 8 weeks were

housed in a controlled animal facility. The ethics approval number is Med-Eth-Re[2022]562. For Fig. 1, the mice were divided into 2 groups, comprising a total of 16 individuals. The AR group received intraperitoneal injections of 50 μg OVA (Sigma-Aldrich) with 1 mg aluminum hydroxide (Thermo Fisher Scientific, Waltham, MA, USA), in a total volume of 200 μL, on days 0, 7, and 14 to induce immunization. Following sensitization, these mice were subjected to intranasal instillation of OVA (10 mg/mL, 20 μL/nostril) for five consecutive days, from day 21 to day 27. In the control group, mice were treated with saline. On day 28, the animals were sacrificed, and nasal mucosa tissues, along with NLF, were collected for further analysis. For Fig. 7, the mice were divided into 4 groups, comprising a total of 32 individuals. For the control and OVA group, the mice were treated the same way as described above. For the OVA + shNC group, a total of 24 h before each OVA challenge on days 21–27, shNC was constructed and intranasally administered to the mice (20 μL; 1×10^8 TU/mL). For the OVA + shSphk1 group, a total of 24 h before each OVA challenge on days 21–27, shSphk1 was constructed and intranasally administered to the mice (20 μL; 1×10^8 TU/mL). On day 28, the animals were sacrificed, and nasal mucosa tissues, along with NLF, were collected for further analysis.

To establish the *in vitro* cell model, hNECs were used. hNECs were cultured in six-well plates until they reached 80–90% confluence, they were washed with PBS and provided with fresh media containing Der p1 (500 ng/mL, Indoor Biotechnologies, Charlottesville, VA, USA) or PBS as a control. The cells were then incubated at 37 °C for 24 h before being utilized for subsequent experiments.

Cell transfection

Cell transfection was conducted following established protocols from previous literature.[22] Briefly, hNECs were seeded 24 h before transfection. Lentiviral-short hairpin RNAs targeting Sphk1 (shSphk1#-1, shSphk1#-2, shSphk1#-3, and shSphk1#-4) and HDAC4 (shHDAC4#-1, shHDAC4#-2, shHDAC4#-3, and shHDAC4#-4), as well as a control shRNA (shNC), were designed by

Thermofisher and inserted into pCDH-CMV-MCS-EF1-Puro vectors by Fenghbio (Changsha, China). The full-length HDAC4 sequence was amplified by PCR and cloned into the pLVX-Puro vector (VT1465, youbio), named OE-HDAC4, and then transfected into hNECs (5×10^6 cells per well). Cells with Sphk1-knockdown or HDAC4-knockdown or HDAC4-overexpression were obtained through puromycin screening.

Enzyme-linked immunosorbent assay (ELISA) assay

Inflammatory markers, IL-18 and IL-1β, in NLF, were assessed with ELISA kits (KHC0181 and KHC0011, Thermo Fisher Scientific) according to the user's manual. ELISA kits were also used to detect IgE (EMIGHE, Thermo Fisher Scientific), IL-4 (BMS613, Thermo Fisher Scientific), HMGB1 (MBS722248, BioSource, San Diego, CA, USA), IL-18 (BMS618-3, Thermo Fisher Scientific) and IL-1β (BMS6002, Thermo Fisher Scientific) expression levels in serum and nasal mucosa tissue according to the user's manual. The absorbance of each well was measured at a wavelength of 450 nm using a spectrophotometer. The concentrations of the contents in each well were then determined by utilizing a standard curve.

Hematoxylin & eosin (HE) staining

The nasal mucosa tissues were fixed in 3.7% formalin, embedded in paraffin, and sliced into 5 μm sections. These sections were then subjected to a 3-min incubation with hematoxylin (Sigma-Aldrich) followed by washing with running tap water for 1 min. Subsequently, the sections were stained with eosin (Sigma-Aldrich) for 45 s. After mounting, images of the stained sections were captured using a Biozero BZ-9000 Series microscope (KEYENCE, Osaka, Japan).

Immunohistochemistry (IHC) staining

The nasal mucosa tissues were immobilized using 3.7% buffered formalin and then encased in paraffin. IHC staining was conducted on 5 μm-thick sections prepared from these encased blocks. The staining protocol followed a previously described procedure.[23] The sections were subjected to incubation with primary antibodies, including Sphk1 (ab262697, 1:1000, Abcam, Cambridge, UK), HMGB1 (ab79823, 1:350, Abcam), ASC
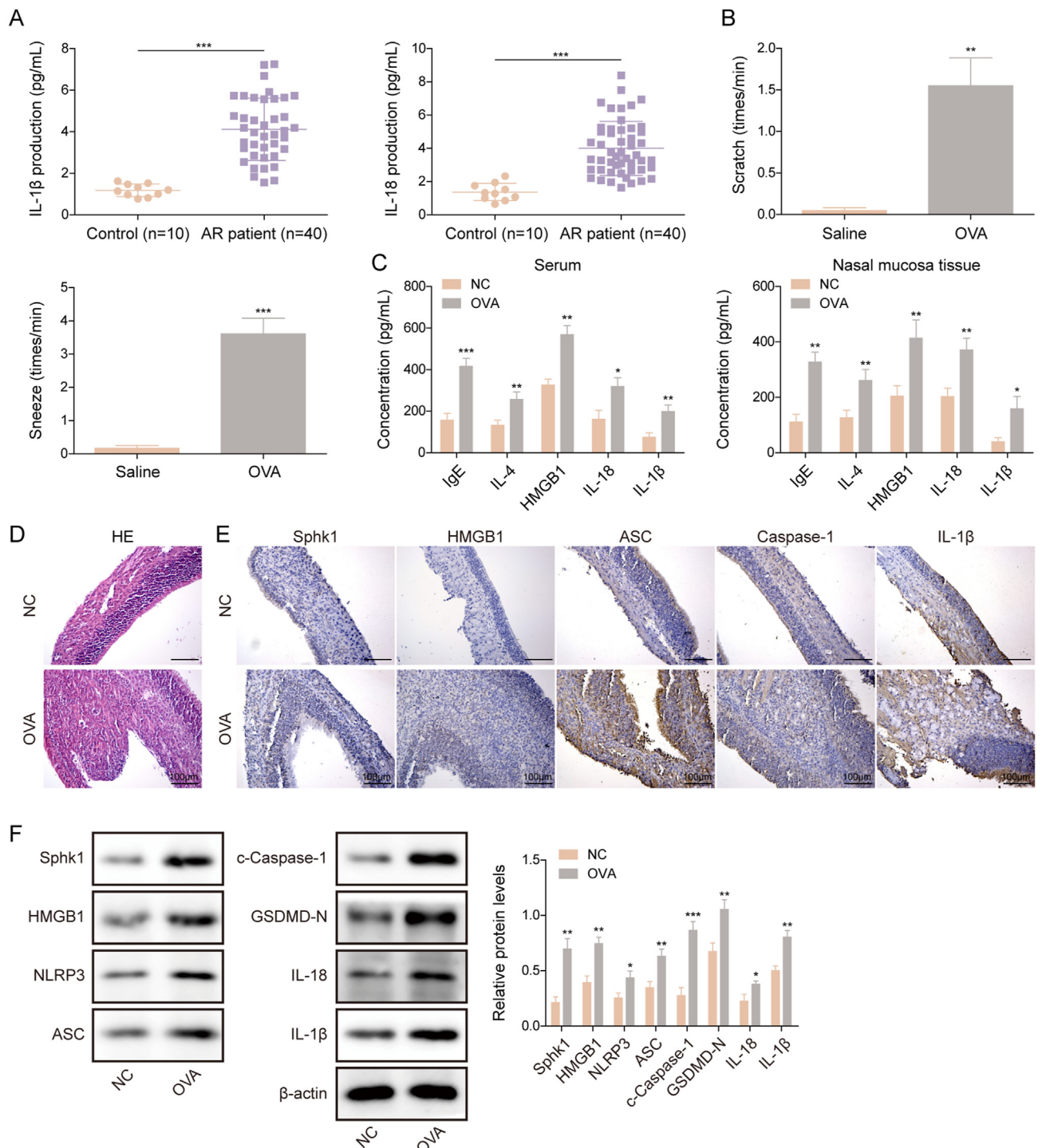
Fig. 1 Sphk1, HMGB1, inflammasome, IL-18 and IL-1β expression was elevated in AR patients and mice. (A) The expression levels of IL-18 and IL-1β were measured in the nasal lavage fluid (NLF) of allergic rhinitis (AR) patients (n = 40) and normal healthy controls (n = 10) using ELISA. Next, an AR mouse model was established using ovalbumin (OVA) (N = 8 per group). (B) The number of scratches and sneezes was recorded in both the AR mouse group and the control group. (C) ELISA was performed to determine the expression levels of IgE, IL-4, HMGB1, IL-18, and IL-1β in the mouse serum and nasal mucosa tissue. (D) HE staining was conducted to evaluate the pathological changes in the mouse nasal mucosal tissue (scale bar = 100 μm). (E) IHC staining was employed to assess the expression levels of Sphk1, HMGB1, ASC, Caspase-1, and IL-1β in the mouse nasal mucosal tissue (scale bar = 100 μm). (F) Western Blot analysis was used to detect the expression levels of Sphk1, HMGB1, NLRP3, GSDMD-N, ASC, c-Caspase-1, IL-1β, and IL-18. *, $P < 0.05$; **, $P < 0.01$; ***, $P < 0.001$

(ab309497, 1:1000, Abcam), and pyroptosis related proteins,[24] including caspase-1 (ab62698 and ab138483, 1:50 and 1000, Abcam), or IL-1β (ab283818, 1:500, Abcam), for 1 h at room temperature. Following this, secondary antibodies were applied. Hematoxylin counterstaining was performed before capturing images using a Leica confocal microscope.

Real-time polymerase chain reaction (RT-qPCR)

qPCR analysis was conducted using the Taqman® Universal PCR Master Mix Kit (Thermo Fisher Scientific, Waltham, MA, USA), with primer sequences procured from Origen Biotech (Wuxi, Jiangsu, China). The $2^{-\triangle\triangle Ct}$ method was employed to quantify relative mRNA levels, which were subsequently normalized to GAPDH.

Western blot

Protein extraction from cells was carried out using radio-immunoprecipitation assay buffer supplemented with protease inhibitors, performed at a temperature of 4 °C for 30 min. The protein concentrations were determined utilizing a BCA protein assay (Thermo Fisher Scientific). 30 μg protein/well was separated by SDS-PAGE and then moved to polyvinylidene fluoride membranes (Merck Millipore, MA, USA). The membranes were blocked, washed with PBS, and incubated with primary antibodies against Sphk1 (ab302714, 1:1000, Abcam), HMGB1 (ab92378, 1:2000, Abcam), HDAC4 (ab32572, 1:5000, Abcam), p-HDAC4 (ab32572, 1:5000, Abcam), pyroptosis related proteins,[24] including NLRP3 (ab40772, 1:1000, Abcam), GSDMD-N (ab76011, 1:5000, Abcam), ASC (ab27568, 1:500, Abcam), Caspase-1 (ab92547, 1:1000, Abcam), IL-1β (ab32572, 1:5000, Abcam), IL-18 (ab32572, 1:5000, Abcam), and the control proteins, β-actin (ab8226, 1:5000, Abcam), and GAPDH (ab8245, 1:500, Abcam), Afterward, the membranes were washed with PBS and incubated with secondary antibodies (A-11001, 1:2000, Invitrogen and 31,402, 1:2000, Invitrogen). Finally, an ECL kit (Merck Millipore) was used to visualize the protein bands.

Immunofluorescent (IF) staining

The cells were fixed using 4% para-formaldehyde (PFA) for approximately 15 min. Subsequently, they were blocked using goat serum and then incubated with primary antibodies targeting pyroptosis-related proteins,[24] including NLRP3 (1:500, AMAb90569, Atlas Antibodies, Lund, Sweden) or Caspase-1 (1:200, PA5-87536, Invitrogen) at 4 °C overnight. Following the primary antibody incubation, the cells were incubated with secondary antibodies (1:1000, ab150113 or ab150077, Abcam). DAPI staining was performed, and the images were captured using a fluorescence microscope (AXIO, Zeiss, Germany).

Flow cytometry

hNECs were treated as described above and were seeded into a dish (Sarstedt, Nümbrecht, Germany) and cultured overnight followed by being loaded with Caspase-1/PI (propidium iodide) probes based on a previously described method.[20] Afterward, cells were incubated with fresh medium for thirty min and trypsinized. Finally, cells were analyzed utilizing flow cytometry (Beckman Coulter Life Sciences, Brea CA, USA) to assess the Caspase-1/PI positive cells, which are considered pyroptotic cells based on the previously published paper.[25]

Co-immunoprecipitation (Co-IP) assay

The interaction of CaMKII-δ and Sphk1 was examined by Co-IP assay. The hNECs were subjected to 2 washes with PBS. Subsequently, the cells were treated with RIP lysis buffer (Merck Millipore). The resulting cell lysates were sonicated on ice in an IP buffer and then centrifuged at 12,000 rpm/min for 10 min. A total of 30 μL of the supernatant was collected as the Input sample. Furthermore, 420 μL of the supernatant was immunoprecipitated overnight at 4 °C with either anti-CaMKII-δ antibody (1:100; PA5-22168, Thermo Fisher Scientific) or control nonspecific IgG antibody (1:1000, ab18413, Abcam). Afterward, protein A was added and incubated for 1 h at 4 °C. Following 4 washes with IP buffer, the sample was centrifuged for 2 min, and the supernatant was discarded. Finally, 30 μL of lysate (2X SDS) was added and incubated for 10 min. Ultimately, the samples were subjected to immunoblotting using either an anti-Sphk1 antibody (ab302714, 1:1000, Abcam) or an anti-CaMKII-δ antibody (1:500; PA5-22168, Thermo Fisher Scientific).

Chromatin immunoprecipitation (ChIP) assay

ChIP assay was used to detect the binding of MEF2C to the HMGB1 promoter. hNECs were harvested and were then treated with RIP lysis buffer (Merck Millipore). Following this, cell cross-linking, and sonication were performed. To the samples, 20 μL of 50 × PIC, 900 μL of ChIP Dilution Buffer, and 60 μL of Protein A Agarose/Salmon SpermDNA were added. After incubation, the samples were centrifuged, and the resulting supernatant was transferred to a separate tube. Subsequently, 1 μL of MEF2C antibody (ab211493, 1:200, Abcam) or IgG antibody (ab205718, 1:1000, Abcam) was added to the supernatant, which was then incubated overnight at 4 °C. After precipitation and subsequent washing steps, 1 μL of RNaseA was added to each tube and incubated at 37 °C for 1 h. To each tube, 10 μL of 0.5 M EDTA, 20 μL of 1 M Tris-HCl, and 2 μL of 10 mg/mL proteinase K were added, followed by incubation at 45 °C for 2 h. The samples were then collected and quantified using Western blot to detect the enrichment of HMGB1 promoter regions, including BS1 and BS2.

Dual-luciferase reporter assay

Dual-luciferase reporter assay was used to detect the binding of MEF2C to the HMGB1 promoter mediated by HDAC4. The experimental procedure followed a published study.[12] In summary, the HMBG1 wild-type sequence (WT) and mutant sequences (MUT-BS1, MUT-BS2, or MUT-BS1&BS2) with alterations in the BS1 and BS2 regions were amplified and inserted into a psi-CHECK2 vector (Promega). Subsequently, HEK293T cells were co-transfected with WT, MUT-BS1, MUT-BS2, or MUT-BS1&BS2 plasmids along with shHDAC4 or corresponding negative control plasmids, using Lipofectamine 2000 transfection reagent (Invitrogen). Following a 48-h incubation period, luciferase activities were assessed using the Dual-Luciferase Reporter Assay Kit from Promega.

Statistical analysis

GraphPad Prism 8.0 was utilized for data analysis in this study. The presented data represent the mean ± standard deviation (SD) and was collected from a minimum of 3 independent experiments. For the comparison of the 2 groups, an unpaired Student's t-test was utilized. In cases involving more than 2 groups, a one-way analysis of variance (ANOVA) followed by the Tukey post hoc test was conducted. A significance threshold of $P < 0.05$ was adopted to determine statistical significance.

RESULTS

Sphk1, HMGB1, inflammasome, IL-18 and IL-1β expression was elevated in AR patients and mice

The expression of IL-18 and IL-1β was found to be upregulated in nasal lavage fluid collected from patients with AR compared to healthy controls (Fig. 1A). Next, we established OVA-induced allergic rhinitis mouse models. The OVA-induced AR mice exhibited a significant increase in the duration of scratching and sneezing per minute compared to the control group (Fig. 1B). Furthermore, the levels of IgE, IL-4, HMGB1, IL-18, and IL-1β in both serum and nasal mucosa tissue were remarkably elevated in the AR mice compared to the control mice (Fig. 1C). HE staining of the nasal mucosa from the AR mice revealed detached cilia and proliferation and expansion of small blood vessels (Fig. 1D). Additionally, IHC staining images of the inferior turbinate mucosal tissue obtained from AR mice demonstrated an increase in the protein expression of Sphk1, HMGB1, Caspase-1, ASC, and IL-1β (Fig. 1E). Western blot analysis further confirmed elevated expression of Sphk1, HMGB1, NLRP3, GSDMD-N, ASC, cleaved Caspase-1 (c-Caspase-1), IL-1β and IL-18 in the inferior turbinate mucosal tissue obtained from AR mice (Fig. 1F). Altogether, the expression of Sphk1, HMGB1, inflammasome, IL-18 and IL-1β was increased in AR mouse models.

Knockdown of Sphk1 inhibited pyroptosis of Der p1-induced nasal epithelial cells (hNECs)

To investigate the role of Sphk1 in regulating the behavior of hNECs in dust mite AR, we conducted knockdown experiments by transfecting sh-Sphk1 into hNECs obtained from dust mite AR patients. The efficiency of transfection was assessed using Western blot analysis. As shown in Fig. 2A, transfection with shSphk1-4# exhibited high efficiency and was therefore chosen for subsequent experiments. To establish an *in vitro* AR
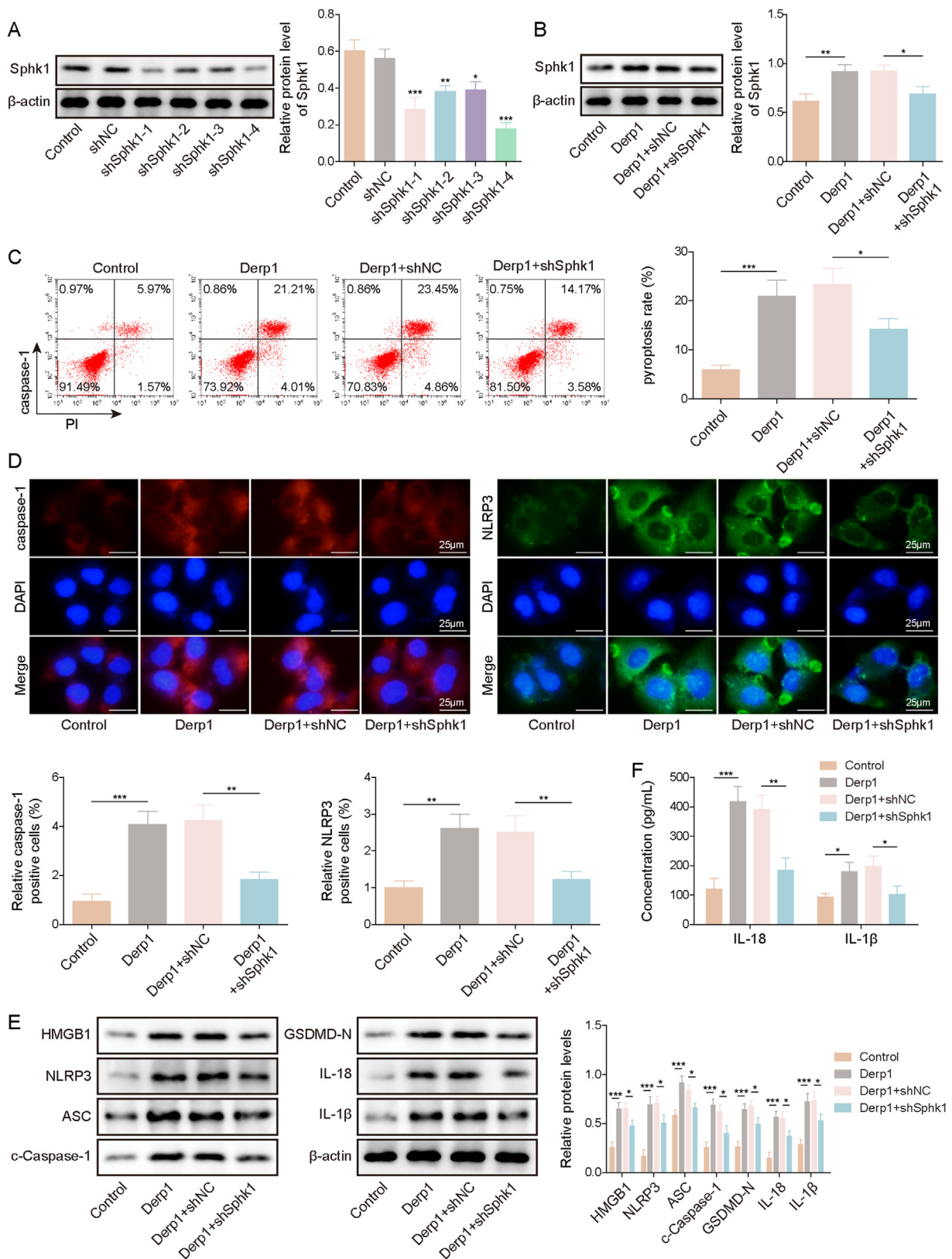
Fig. 2 Knockdown of Sphk1 inhibited pyroptosis of Der p1-induced nasal epithelial cells. (A) Nasal epithelial cells (hNECs) were obtained from dust mite AR patients. Establish Sphk1 knockdown hNECs cells and assess the expression of Sphk1 using Western blot. *An in vitro* cell model of AR was established using dust mite protein Der p1 and then Sphk1 was knocked down in the AR cell model. (B) The expression of Sphk1 was determined using Western blot. (C) Flow cytometry detected the percentage of Caspase-1/PI-positive cells. (D) IF staining assessed the expression of Caspase-1 and NLRP3 (scale bar = 25 μm). (E) Western Blot measured the expression levels of HMGB1,

model, hNECs were treated with Der p1, followed by transfection with shSphk1-4#. Treatment with Der p1 significantly increased Sphk1 expression in hNECs, which was attenuated by Sphk1 knockdown (Fig. 2B). The percentage of Caspase-1/PI positive cells was significantly elevated in Der p1-induced hNECs (Fig. 2C), while silencing Sphk1 had the opposite effect. IF staining images and Western blot analysis showed that Der p1 treatment markedly increased Caspase-1 and NLRP3 expression. However, the upregulation of Caspase-1 and NLRP3 expression induced by Der p1 treatment was reversed by Sphk1 depletion (Fig. 2D). Additionally, the protein levels of HMGB1, NLRP3, c-Caspase-1, ASC, GSDMD-N, IL-18, and IL-1β were elevated in Der p1-induced hNECs, and this elevation was reversed by Sphk1 knockdown (Fig. 2E). The secretion of IL-18 and IL-1β was also enhanced in Der p1-treated hNECs, as detected by ELISA. However, knocking down Sphk1 diminished the secretion of IL-18 and IL-1β induced by Der p1 treatment (Fig. 2F). In conclusion, silencing Sphk1 attenuated pyroptosis in hNECs induced by Der p1 treatment.

HDAC4 overexpression suppressed Der p1-induced nasal mucosal epithelial cell pyroptosis through the regulation of HMGB1

To investigate the role of HDAC4 in regulating the pyroptosis of hNECs in dust mite-induced AR, we overexpressed HDAC4 in hNECs obtained from dust mite AR patients. The efficiency of transfection was confirmed through Western blot analysis (Fig. 3A). Next, hNECs were treated with Der p1, followed by overexpression of HDAC4. Der p1 treatment significantly reduced HDAC4 expression in hNECs, which was restored by HDAC4 overexpression (Fig. 3B). HDAC4 overexpression notably inhibited Der p1-induced Caspase-1/PI positive cells, indicating the suppression of pyroptosis (Fig. 3C). Furthermore, the upregulation of Caspase-1 and NLRP3 expression induced by Der p1 treatment was reversed by HDAC4 overexpression (Fig. 3D). Additionally, HDAC4 overexpression counteracted the Der p1-induced elevation of protein levels of HMGB1, NLRP3, c-Caspase-1, ASC, GSDMD-N, IL-18, and IL-1β

(Fig. 3E). The secretion of IL-18 and IL-1β, induced by Der p1 treatment, was diminished upon HDAC4 overexpression (Fig. 3F). The findings above suggest that HDAC4 overexpression attenuated Der p1-induced pyroptosis of hNECs through the regulation of HMGB1.

HDAC4 mediated the transcription of HMGB1 via MEF2C

To validate the regulatory role of HDAC4 in HMGB1-mediated pyroptosis of hNECs, we performed knockdown experiments by transfecting sh-HDAC4 into Der p1-induced hNECs. The efficiency of transfection was assessed using Western blot analysis. As depicted in Fig. 4A, transfection with shHDAC4-2# exhibited high efficiency and was selected for subsequent experiments. Knockdown of HDAC4 significantly induced the expression of HMGB1 (Fig. 4A). According to the bioinformatic prediction tool AnimalTFDB (http://bioinfo.life.hust.edu.cn/AnimalTFDB/#!/), the transcription factor MEF2C, which interacts with HDAC4, was predicted to bind to specific regions of the HMGB1 promoter, including BS1 and BS2 (Fig. 4B). Anti-MEF2C antibody greatly enriched BS1 and BS2 fragments of the HMGB1 promoter, further confirming that MEF2C bound to the HMGB1 promoter (Fig. 4C). Knockdown of HDAC4 increased luciferase activity of MEF2C to the HMGB1 promoter. However, when the BS1 or BS2 regions were mutated, there was minimal change in luciferase activity. Intriguingly, when both BS1 and BS2 were mutated, luciferase activity decreased (Fig. 4D). Overexpression of HDAC4 resulted in a decrease in the activity of MEF2C binding to the HMGB1 promoter. Conversely, in an *in vitro* AR model, the downregulation of HDAC4 mediated by Der p1 increased the activity of MEF2C binding to the HMGB1 promoter, thereby reversing the decrease in dual-luciferase activity caused by HDAC4 overexpression (Fig. 4E).

Collectively, these findings demonstrate that HDAC4 mediated the transcriptional regulation of HMGB1 through MEF2C in Der p1-induced hNECs.
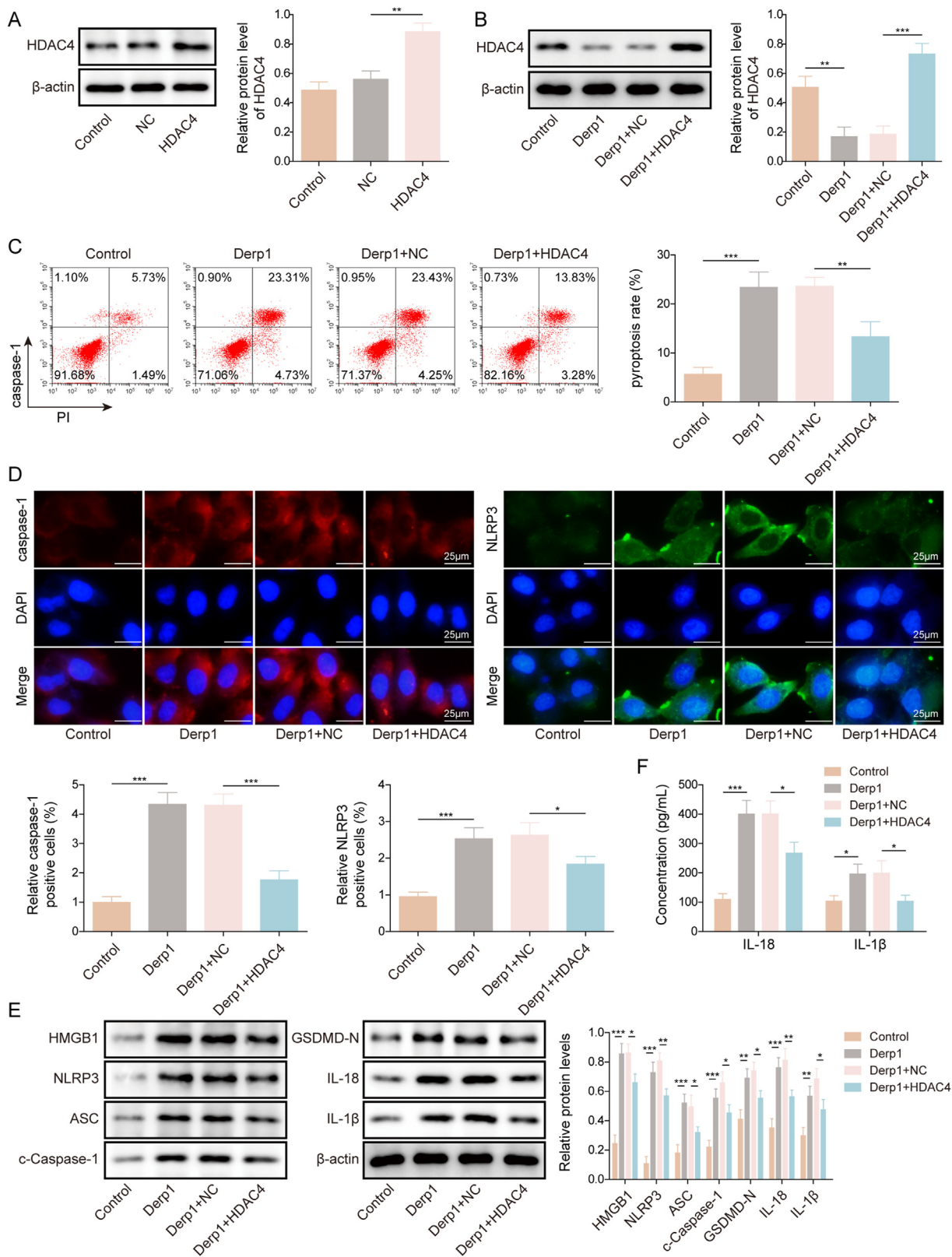

NLRP3, GSDMD-N, ASC, c-Caspase-1, IL-1β, and IL-18. (F) ELISA examined the protein levels of IL-18, and IL-1β. All experiments were repeated at least three times. *, $P < 0.05$; **, $P < 0.01$; ***, $P < 0.001$

Fig. 3 HDAC4 overexpression suppressed Der p1-induced nasal mucosal epithelial cell pyroptosis through the regulation of HMGB1. (A) Nasal epithelial cells (hNECs) were obtained from dust mite AR patients. Established HDAC4 overexpressed hNECs and assessed the expression of HDAC4 using Western blot. *The in vitro* cell model of AR was established by treating the hNECs without or with dust mite protein Der p1. Afterward, HDAC4 was overexpressed in the AR cell model. (B) The expression of HDAC4 was determined using Western blot. (C) Flow cytometry detected the percentage of Caspase-1/PI-positive cells. (D) IF staining assessed the expression of
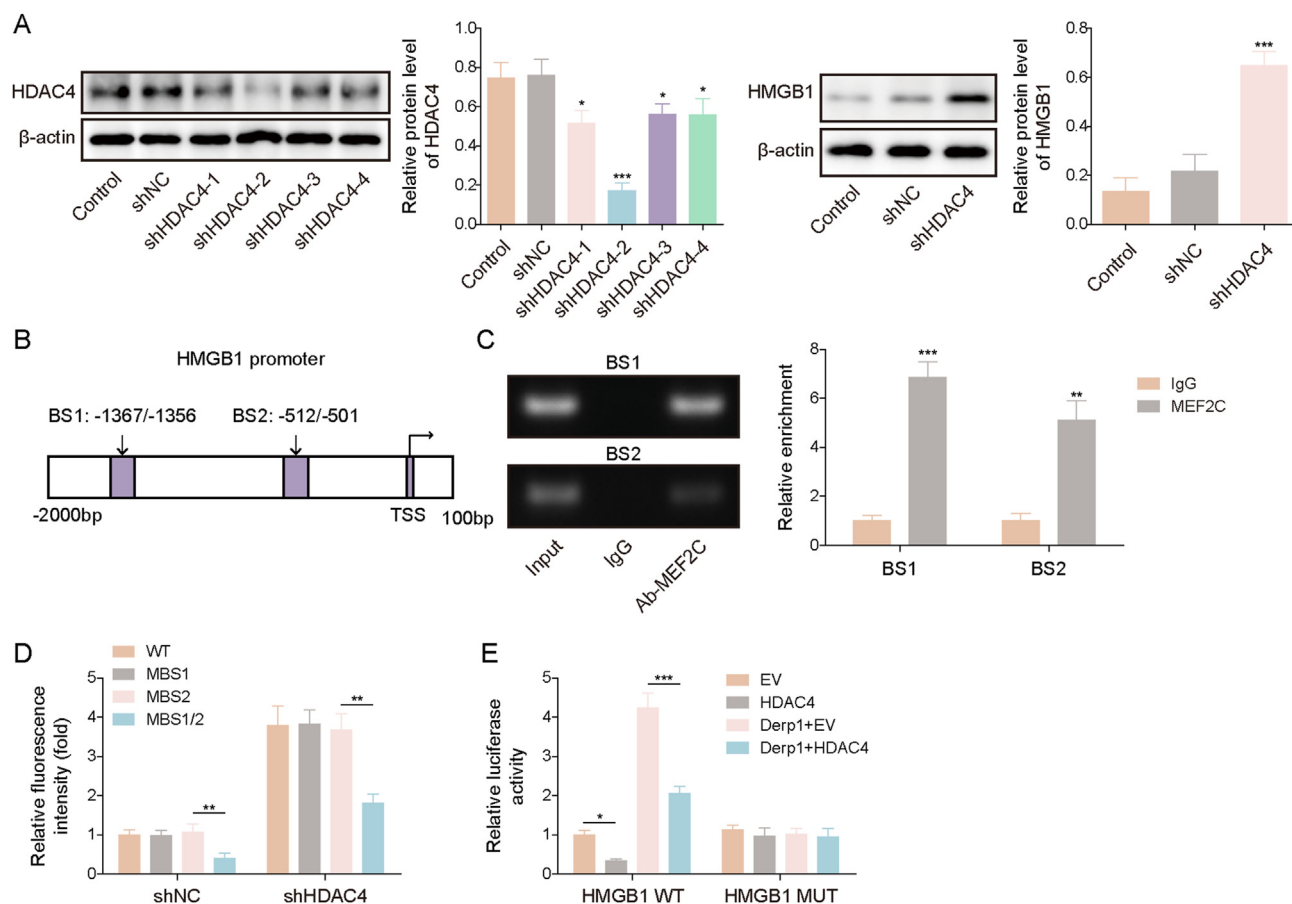
Fig. 4 HDAC4 mediated the transcription of HMGB1 via MEF2C. (A) Nasal epithelial cells (hNECs) were obtained from dust mite AR patients. Established HDAC4-depleted hNECs cells and assessed the expression of HDAC4 and HMGB1 using Western blot. (B) Bioinformatics analysis predicted the binding of MEF2C to the HMGB1 promoter. (C–D) ChIP and dual-luciferase reporter assay investigated the binding of MEF2C to the HMGB1 promoter. (E) Der p1 was used to treat hNECs to induce the *in vitro* AR model. Afterward, the dual-luciferase reporter assay investigated the binding of MEF2C to the HMGB1 promoter through HDAC4. All experiments were repeated at least three times. *, $P < 0.05$; **, $P < 0.01$; ***, $P < 0.001$

Sphk1 directly interacted with CaMKII-δ to promote the phosphorylation of HDAC4 and inhibited the cytoplasmic translocation of HDAC4 to the nucleus in *in vitro* AR model

Previous studies have demonstrated that Sphk1 binds to CaMKII-δ and mediates the phosphorylation and translocation of HDAC4 in Kupffer cells. Here, we sought to examine the influence of Sphk1 inhibition on HDAC4 translocation in an *in vitro* AR model. Treatment with Der p1 resulted in an increased protein level of HDAC4 in the cytoplasm, rather than the nucleus (Fig. 5A). However, the addition of the Sphk1 inhibitor SKI-5C

reversed this effect. Furthermore, Der p1 treatment inhibited the cytoplasmic translocation of HDAC4 to the nucleus in hNECs, which was restored by SKI-5C (Fig. 5B). In the AR model, the expression of phosphorylated HDAC4 (p-HDAC4) was elevated (Fig. 5C). Conversely, the introduction of the Sphk1 inhibitor SKI-5C led to a reduction in the expression of p-HDAC4. The primary mechanism driving the translocation of HDAC4 from the nucleus to the cytoplasm is phosphorylation, and it is known that the phosphorylation of HDAC4 is modulated by calcium/calmodulin-dependent kinase II-δ (CaMKII-δ). Fig. 5D demonstrates a significant reduction in Der
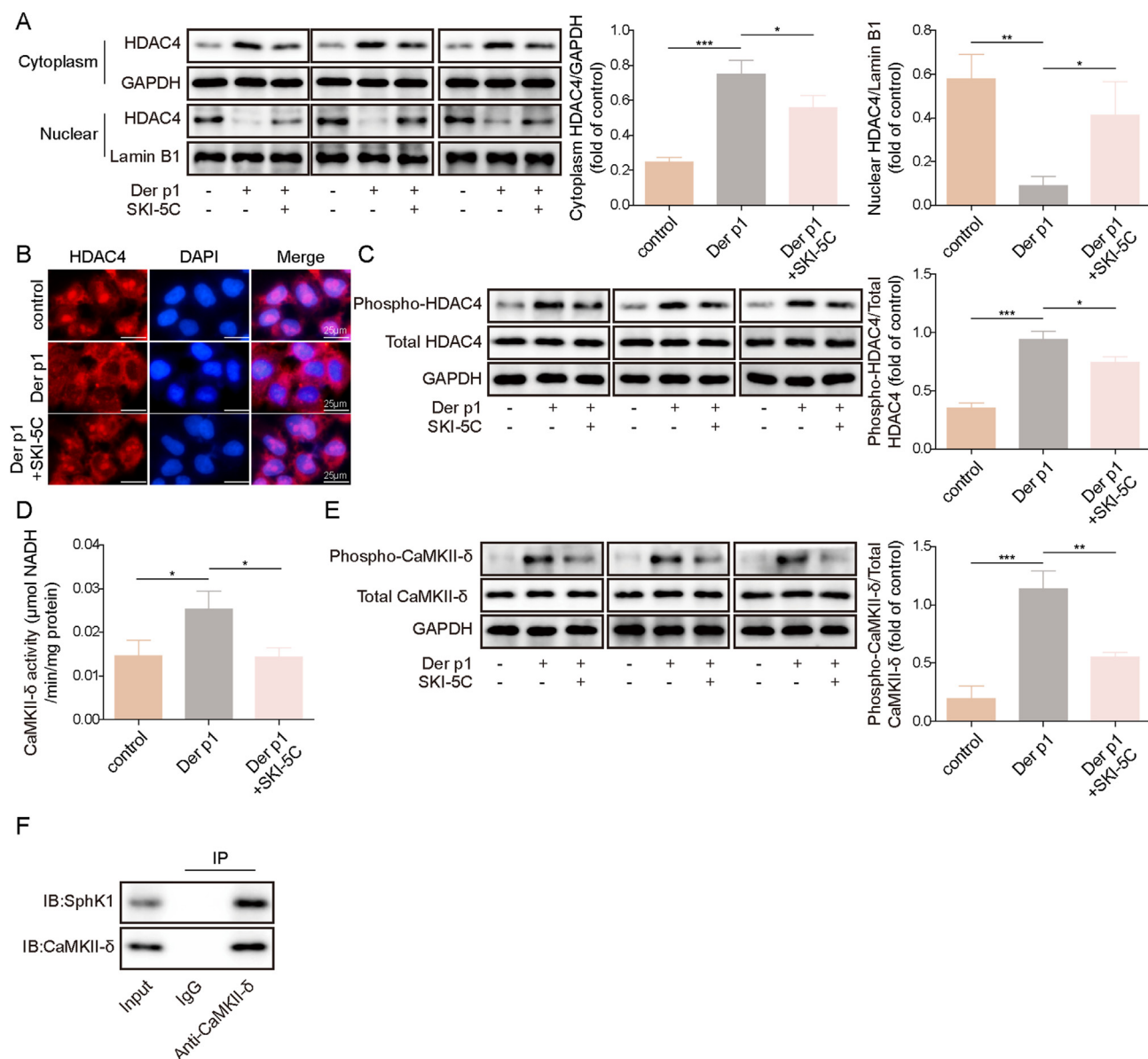
Fig. 5 Sphk1 directly interacted with CaMKII-δ to promote the phosphorylation of HDAC4 and inhibited the cytoplasmic translocation of HDAC4 to the nucleus in *in vitro* AR model. Nasal epithelial cells (hNECs) were obtained from dust mite AR patients. hNECs were treated without or with Der p1 or Der p1/Sphk1 inhibitor, SKI-5C. (A) Cytoplasm HDAC4 and nuclear HDAC4 expression were assessed via Western blot. (B) IF staining illustrated HDAC4 expression (scale bar = 25 μm). (C) Western blot detected phosphorylated HDAC4 and total HDAC4 expression levels. (D) CaMKII-δ activity was measured. (E) Western blot examined phosphorylated CaMKII-δ and total CaMKII-δ expression. (F) Co-IP assay investigated the interaction between Sphk1 and CaMKII-δ in hNECs. All experiments were repeated at least three times. *, $P < 0.05$; **, $P < 0.01$; ***, $P < 0.001$

p1-activated CaMKII-δ upon Sphk1 inhibition. The phosphorylation of CaMKII-δ induced by Der p1 treatment was reversed by SKI-5C (Fig. 5E). Importantly, *in vitro* Co-IP assays revealed a potential direct interaction between Sphk1 and CaMKII-δ (Fig. 5F).

In summary, the binding of Sphk1 to CaMKII-δ promoted the activity of CaMKII-δ, leading to an increase in the activity of phosphorylated HDAC4,

which inhibited the cytoplasmic translocation of HDAC4 to the nucleus in *in vitro* AR model.

Downregulation of HDAC4 reversed the effect of Sphk1 knockdown on Der p1-induced nasal mucosal epithelial cell pyroptosis

We next knocked down Sphk1 or/and HDAC4 in Der p1-induced hNECs to further elucidate the regulatory role of Sphk1 and HDAC4 on nasal
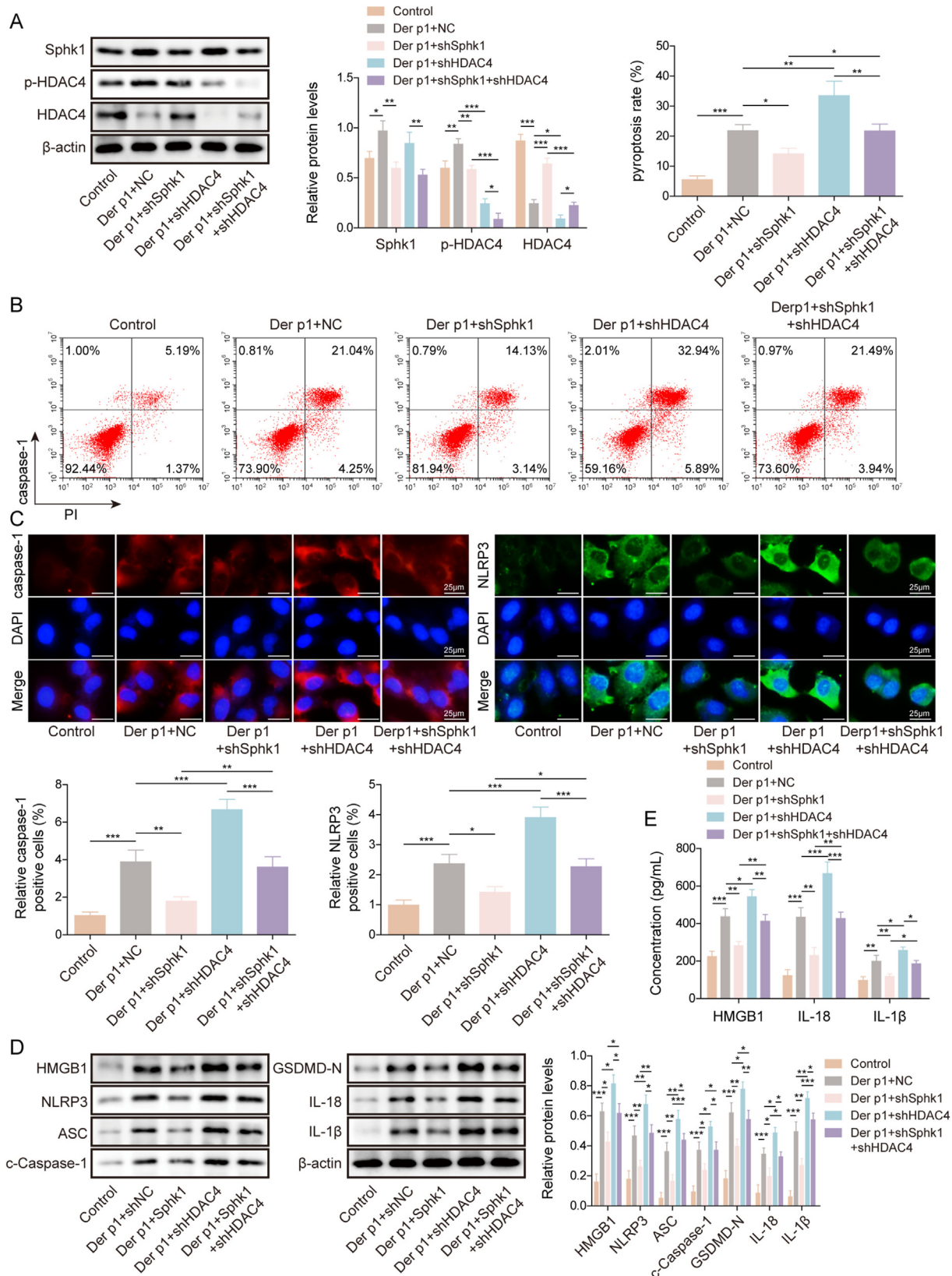
Fig. 6 Downregulation of HDAC4 reversed the protective effect of Sphk1 knockdown on Der p1-induced nasal mucosal epithelial cell pyroptosis. Nasal epithelial cells (hNECs) were obtained from dust mite AR patients. hNECs were treated without or with Der p1. Afterward, Sphk1 and HDAC4 were knocked down by transfecting the Der p1-treated cells with shSphk1-4# and shHDAC4-2#, respectively. (A) The expression of Sphk1, HDAC4, and phosphorylated HDAC4 was determined using Western blot. (B) Flow cytometry detected the

mucosal epithelial cell pyroptosis. Silencing Sphk1 reversed the upregulation of Sphk1 and phosphorylation of HDAC4 induced by Der p1 and restored the inhibitory effect of Der p1 on HDAC4 expression (Fig. 6A). Knockdown of HDAC4 further reduced phosphorylation of HDAC4 and HDAC4 expression in both Der p1-induced hNECs and Der p1-treated plus Sphk1-depleted hNECs (Fig. 6A). Knockdown of HDAC4 reversed the inhibitory effect of Sphk1 depletion on the percentage of Caspase 1/PI positive cells (Fig. 6B). Additionally, the downregulation of Caspase-1 and NLRP3 expression induced by Sphk1 knockdown in Der p1-treated hNECs was reversed by HDAC4 depletion (Fig. 6C). Moreover, silencing HDAC4 counteracted the decrease in protein levels of HMGB1, NLRP3, ASC, c-Caspase-1, GSDMD-N, IL-18, and IL-1β induced by Sphk1 knockdown (Fig. 6D). The decrease in HMGB1, IL-18 and IL-1β secretion resulting from Sphk1 downregulation was diminished upon shHDAC4 transfection (Fig. 6E). Altogether, the silencing of HDAC4 restored the inhibitory effect of Sphk1 knockdown on Der p1-induced pyroptosis of hNECs.

Suppression of Sphk1 reduced HMGB1-regulated nasal mucosal epithelial cell pyroptosis in AR mouse models

To validate the regulatory effect of Sphk1 and HMGB1 on nasal mucosal epithelial cell pyroptosis in an *in vivo* AR model, we conducted further experiments. Firstly, we treated mice with OVA and subsequently intranasally injected shSphk1 or shNC. Following OVA administration, there was a significant increase in the frequency of scratching and sneezing compared to the control group, which was reversed by Sphk1 depletion (Fig. 7A). The elevation of protein levels of IgE, IL-4, HMGB1, IL-18, and IL-1β induced by OVA in serum and nasal mucosa tissue was diminished upon Sphk1 knockdown (Fig. 7B). Histological examination of the nasal mucosa using HE staining revealed detached cilia and proliferation and expansion of small blood vessels in AR mice, while in Sphk1-depleted AR mice, a pseudostratified ciliated columnar epithelium composed primarily of ciliated columnar epithelial cells and goblet cells with only a few blood vessels was observed (Fig. 7C). Furthermore, IHC staining of inferior turbinate mucosal tissue demonstrated that Sphk1 depletion reversed the OVA-induced increase in the protein expression of Sphk1, HMGB1, Caspase-1, ASC, and IL-1β (Fig. 7D). Western blot analysis further confirmed that downregulation of Sphk1 attenuated the OVA-induced expression of Sphk1, HMGB1, NLRP3, GSDMD-N, ASC, Caspase-1, IL-1β, and IL-18 in the inferior turbinate mucosal tissue (Fig. 7E). Taken together, silencing of Sphk1 significantly attenuated HMGB1-mediated pyroptosis of hNECs in AR mice.

DISCUSSION

Pyroptosis has been identified as a significant contributor to the development of AR and specific drugs have displayed promising potential in treating AR by targeting the inhibition of pyroptosis. [1] Despite these advancements, the precise underlying mechanism of pyroptosis in AR still requires further investigation. This study demonstrates that in both AR patients and mouse models, there was an elevation in the expression of Sphk1 and HMGB1 as well as pyroptosis-related inflammasome components and the pro-inflammatory cytokines. Silencing of Sphk1 inhibited Der p1-induced hNEC pyroptosis *in vitro* and mouse AR model *in vivo*. We also showed that Sphk1 interacted with CaMKII-δ to facilitate the phosphorylation of HDAC4, which prevented its translocation from the cytoplasm to the nucleus in hNECs. Furthermore, this cellular mechanism allowed HDAC4 reduction in the nucleus to bind to the promoter region of HMGB1 via MEF2C, leading to the upregulation of HMGB1 expression, thereby inducing pyroptosis-mediated inflammation and AR. The study provides important insights into the molecular mechanisms underlying Sphk1-regulated hNEC pyroptosis and highlights a potential therapeutic target Sphk1 and HMGB1 for AR treatment.

Sphk1 was well-accepted to play a critical role in regulating inflammatory responses.[26] For example, The Sphk1/S1P/S1PR2 axis was found
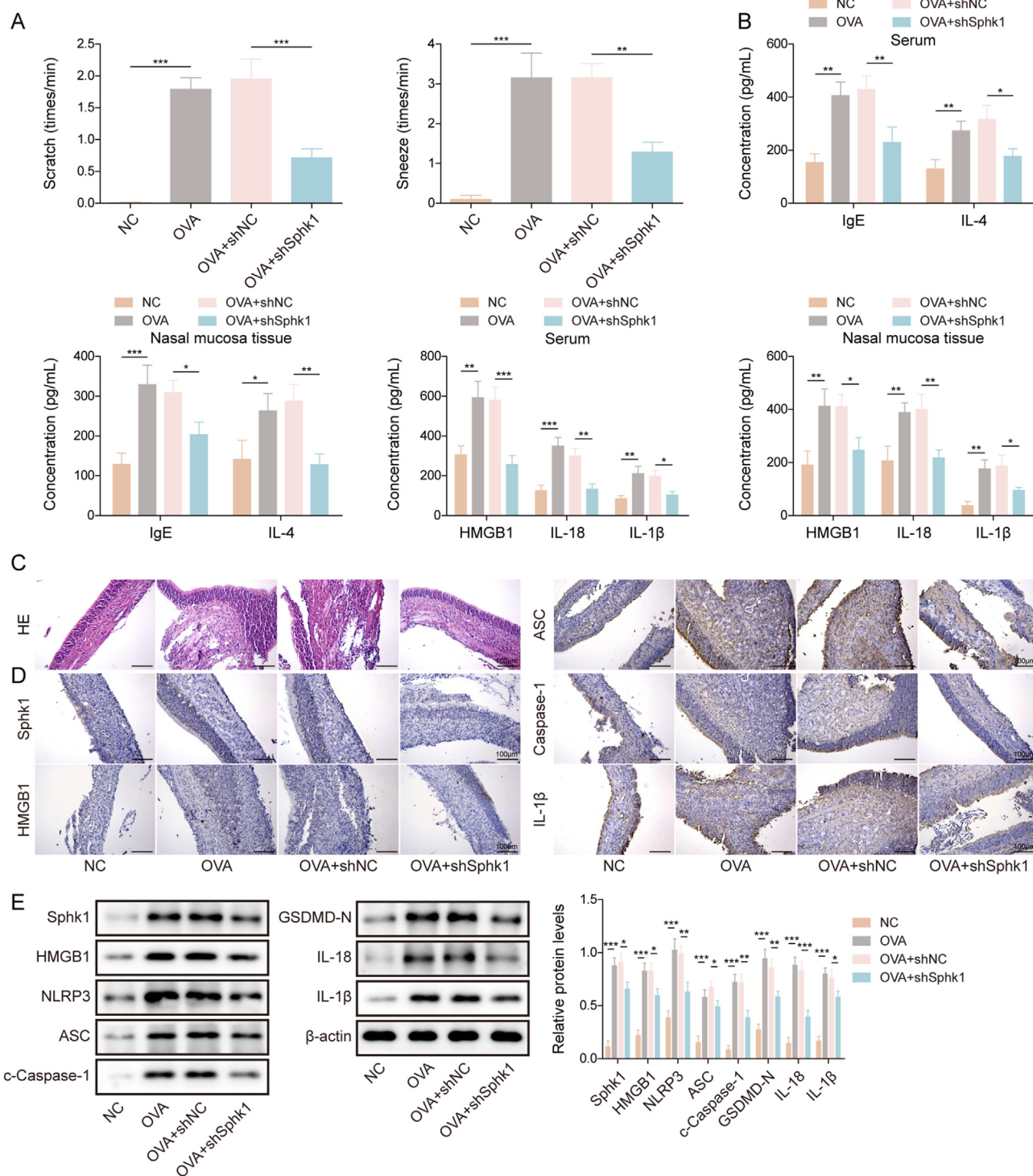
Fig. 7 Suppression of Sphk1 reduced HMGB1-regulated nasal mucosal epithelial cell pyroptosis in AR mouse models. Female BALB/c mice between seven and eight weeks were treated with ovalbumin (OVA) to establish the AR mouse model. Afterward, shSphk1 or negative control (shNC) was established and subcutaneously injected into mice. (A) The number of scratches and sneezes per minute was recorded in different mouse groups. (B) ELISA detected serum and nasal mucosa tissue protein levels of IgE, IL-4, HMGB1, IL-18 and IL-1β. (C) HE staining was performed to examine the pathological changes in the inferior turbinate mucosal tissue collected from different mouse groups (scale bar = 100 μm). (D) IHC staining was used to assess the expression levels of Sphk1, HMGB1, ASC, Caspase-1, and IL-1β in the inferior turbinate mucosal tissue collected from different mouse groups (scale bar = 100 μm). (E) Western Blot analysis was used to detect the expression levels of Sphk1, HMGB1, NLRP3, GSDMD-N, ASC, c-Caspase-1, IL-1β, and IL-18 in the inferior turbinate mucosal tissue collected from different mouse groups. N = 8 for per group. *, $P < 0.05$; **, $P < 0.01$; ***, $P < 0.001$

to regulate the NLRP3 inflammasome and promote pyroptosis by activating NF-κB in human pulmonary artery smooth muscle cells.[27] Previous studies showed that S1P produced by Sphk1 plays a significant role in AR.[18] In a murine AR model, inhibiting S1P and sphingosine lyase effectively suppressed the development of the allergic condition.[28] However, the specific role of Sphk1 in AR has not yet been extensively studied in the literature. In this present study, we demonstrated that Sphk1, HMGB1, and pyroptosis-related indicators, including NLRP3, Caspase-1, GSDMD-N, IL-1β, and IL-18 were significantly upregulated in both AR patients and mouse models. Knockdown of Sphk1 significantly suppressed Der p1-induced hNEC pyroptosis by inhibiting HMGB1. In agreement with our study, other research has also documented the regulatory relationship between Sphk1 and HMGB1. Tian et al found that suppressing Sphk1 resulted in reduced HMGB1 expression in Kupffer cells.[15] Another separate study demonstrated that inhibiting Sphk1 led to the improvement of acute liver failure, primarily attributed to the reduction of HMGB1 cytoplasmic translocation in liver cells.[29] These findings collectively support the importance of Sphk1 in the regulation of HMGB1.

Previous research indicated that in sepsis-associated liver injury, the intracellular shift of HDAC4 mediated the translocation of HMGB1.[15] Spinal nerve ligation and behavioral allodynia induced HDAC4 phosphorylation and accumulation in the cytoplasm, which suppressed the transcription of the HMGB1 gene and resulted in enhanced HMGB1 expression in rats.[30] These studies suggest that HDAC4 plays a critical role in mediating HMGB1 expression. In addition, HDAC activity is recognized as a critical factor in sustaining allergic inflammation and promoting tight junction dysfunction.[31] The depletion of HDAC4 led to the improvement of IL-13-triggered inflammatory response and mucus production in NECs through the activation of the SIRT1/NF-κB signaling pathway. Therefore, we also investigated the role of HDAC4 in Sphk1/HMGB1-regulated pyroptosis and AR. Consistently, HDAC4 was identified as a mediator of HMGB1 transcriptional regulation in our study. Its overexpression effectively suppressed HMGB1-induced pyroptosis in hNECs. Notably, we also

established, for the first time, that HDAC4 exerted its mediating influence on HMGB1 through direct interaction with the transcription factor MEF2C in hNECs.

The activity of HDAC4 is controlled through its subcellular localization.[19] HDAC4 can shuttle between the nucleus and cytoplasm in response to specific stimuli, constituting the primary mechanism that regulates its enzymatic activity.[32] In a previous study, it was revealed that Sphk1 directly interacted with CaMKII-δ to modulate the phosphorylation and intracellular shift of HDAC4 in sepsis-associated liver injury.[15] Additionally, research has shown that CaMKII-δ regulated HDAC4 phosphorylation, leading to increased nuclear export, decreased nuclear import of HDAC4, and subsequent suppressed HDAC4 target genes.[33] In agreement with this, we found that Sphk1 interacted with CaMKII-δ to facilitate the phosphorylation of HDAC4, effectively impeding its translocation to the nucleus. As a result, the reduced nuclear presence of HDAC4 led to increased HMGB1 expression and promoted hNEC pyroptosis.

The primary shortcoming of this study is that it focused mainly on dust mite-induced AR, raising the question of whether the findings are applicable to other allergens or forms of AR. Future research should aim to validate these findings across various allergens and forms of AR to determine their broader applicability. Another limitation is the relatively limited number of samples due to time and funding restrictions.

In summary, this study highlights the crucial role of Sphk1 in promoting AR through its interaction with CaMKII-δ and subsequent regulation of HDAC4 and HMGB1. By elucidating this pathway, we have identified potential novel targets for therapeutic intervention, offering hope for more effective treatments for AR in the future.

Abbreviations

ANOVA, one-way analysis of variance; ATCC, American Type Culture Collection; AR, allergic rhinitis; ASC, apoptosis-associated speck-like protein containing a CARD; ChIP, chromatin immunoprecipitation; DMEM, Dulbecco's Modified Eagle Medium; Sphk1, sphingosine kinase 1; CaMKII-δ, calcium/calmodulin-dependent protein kinase II; Co-IP, co-immunoprecipitation; ELISA, enzyme-linked immunosorbent assay; FBS, fetal bovine serum; HE,

hematoxylin & eosin; hNECs, human nasal epithelial cells; HDAC4, histone deacetylase 4; HMGB1, high mobility group box 1; IF, immunofluorescent; IHC, immunohisto-chemistry; NLRP3, NOD-like receptor family pyrin domain-containing protein 3; NLF, nasal lavage fluid; OVA, oval-bumin; PBS, phosphate-buffered saline; PFA, para-formaldehyde; RT-qPCR, real-time polymerase chain reaction; S1P, sphingosine 1-phosphate.

Availability of data and materials
The datasets generated during and/or analyzed during the current study are available from the corresponding author on reasonable request.

Authors' contributions
Wei Huang: Conceptualization; Writing - Original Draft; Supervision.
Xi Chen: Methodology; Validation; Funding acquisition.
Zizhen Liu: Formal analysis.
Changwu Li: Data Curation.
Xin Wei: Resources.
Jiabin Zhan: Investigation.
Quan Qiu: Visualization.
Jing Zheng: Writing - Review & Editing; Project administration.

Ethics approval and consent to participate
Written informed content was received from each patient. The study was proved by Hainan General Hospital, Hainan Affiliated Hospital of Hainan Medical University. This study received ethical approval from Hainan General Hospital, Hainan Affiliated Hospital of Hainan Medical University for all animal experiments conducted. Ethics approval: Med-Eth-Re[2022]562.

Consent for publication
The informed consent was obtained from study participants.

Authors' consent for publication
All the authors have read and approved the final version for publication in WAO Journal.

Declaration of competing interest
No conflicts of interest, financial or otherwise, are declared by the authors.

Author details
Department of Otorhinolaryngology Head and Neck Surgery, Hainan General Hospital, Hainan Affiliated Hospital of Hainan Medical University, Haikou 570311, Hainan Province, PR China.

REFERENCES

1. Cheng N, Wang Y, Gu Z. Understanding the role of NLRP3-mediated pyroptosis in allergic rhinitis: a review. *Biomed Pharmacother*. 2023;165, 115203.

2. Nur Husna SM, Tan HT, Md Shukri N, Mohd Ashari NS, Wong KK. Allergic rhinitis: a clinical and pathophysiological overview. *Front Med (Lausanne)*. 2022;9:874114.

3. Bousquet J, Melén E, Haahtela T, et al. Rhinitis associated with asthma is distinct from rhinitis alone: the ARIA-MeDALL hypothesis. *Allergy*. 2023;78(5):1169–1203.

4. Yang Z, Liang C, Wang T, et al. NLRP3 inflammasome activation promotes the development of allergic rhinitis via epithelium pyroptosis. *Biochem Biophys Res Commun*. 2020;522(1):61–67.

5. Kelley N, Jeltema D, Duan Y, He Y. The NLRP3 inflammasome: an overview of mechanisms of activation and regulation. *Int J Mol Sci*. 2019;20(13):3328.

6. He Y, Hara H, Núñez G. Mechanism and regulation of NLRP3 inflammasome activation. *Trends Biochem Sci*. 2016;41(12): 1012–1021.

7. Wang R, Wang Y, Yang Q, et al. Xiaoqinglong decoction improves allergic rhinitis by inhibiting NLRP3-mediated pyroptosis in BALB/C mice. *J Ethnopharmacol*. 2024;321: 117490.

8. Zhou H, Zhang W, Qin D, et al. Activation of NLRP3 inflammasome contributes to the inflammatory response to allergic rhinitis via macrophage pyroptosis. *Int Immunopharm*. 2022;110:109012.

9. Jiao B, Guo S, Yang X, et al. The role of HMGB1 on TDI-induced NLPR3 inflammasome activation via ROS/NF-κB pathway in HBE cells. *Int Immunopharm*. 2021;98:107859.

10. Yuan S, Liu Z, Xu Z, Liu J, Zhang J. High mobility group box 1 (HMGB1): a pivotal regulator of hematopoietic malignancies. *J Hematol Oncol*. 2020;13(1):91.

11. Hou C, Zhao H, Liu L, et al. High mobility group protein B1 (HMGB1) in Asthma: comparison of patients with chronic obstructive pulmonary disease and healthy controls. *Mol Med*. 2011;17(7–8):807–815.

12. Zhu X, Cong J, Yang B, Sun Y. Association analysis of high-mobility group box-1 protein 1 (HMGB1)/toll-like receptor (TLR) 4 with nasal interleukins in allergic rhinitis patients. *Cytokine*. 2020;126:154880.

13. Bellussi LM, Cocca S, Chen L, Passali FM, Sarafoleanu C, Passali D. Rhinosinusal inflammation and high mobility group box 1 protein: a new target for therapy. *ORL J Otorhinolaryngol Relat Spec*. 2016;78(2):77–85.

14. Chen R, Kang R, Tang D. The mechanism of HMGB1 secretion and release. *Exp Mol Med*. 2022;54(2):91–102.

15. Tian T, Yao D, Zheng L, et al. Sphingosine kinase 1 regulates HMGB1 translocation by directly interacting with calcium/

calmodulin protein kinase II-δ in sepsis-associated liver injury. *Cell Death Dis*. 2020;11(12):1037.

16. Bu Y, Wu H, Deng R, Wang Y. Therapeutic potential of SphK1 inhibitors based on abnormal expression of SphK1 in inflammatory immune related-diseases. *Front Pharmacol*. 2021;12:733387.

17. Wang X, Yang Y, Cai WQ, Lu Y. The relationship of sphingosine kinase 1 with pyroptosis provides a new strategy for tumor therapy. *Front Immunol*. 2020;11:574990.

18. Kulinski JM, Muñoz-Cano R, Olivera A. Sphingosine-1-phosphate and other lipid mediators generated by mast cells as critical players in allergy and mast cell function. *Eur J Pharmacol*. 2016;778:56–67.

19. Wang Z, Qin G, Zhao TC. HDAC4: mechanism of regulation and biological functions. *Epigenomics*. 2014;6(1):139–150.

20. Xu H, Wang L, Chen H, Cai H. HDAC4 depletion ameliorates IL-13-triggered inflammatory response and mucus production in nasal epithelial cells via activation of SIRT1/NF-κB signaling. *Immun Inflamm Dis*. 2022;10(11):e692.

21. Fawcett LK, Turgutoglu N, Allan KM, et al. Comparing cytology brushes for optimal human nasal epithelial cell collection: implications for airway disease diagnosis and research. *J Pers Med*. 2023;13(5).

22. Pan Y, Zhang Y, Liu W, et al. LncRNA H19 overexpression induces bortezomib resistance in multiple myeloma by targeting MCL-1 via miR-29b-3p. *Cell Death Dis*. 2019;10(2):106.

23. Koukourakis MI, Giatromanolaki A, Sivridis E, et al. LYVE-1 immunohistochemical assessment of lymphangiogenesis in endometrial and lung cancer. *J Clin Pathol*. 2005;58(2):202–206.

24. Zhang X, Wang Q, Cao G, Luo M, Hou H, Yue C. Pyroptosis by NLRP3/caspase-1/gasdermin-D pathway in synovial tissues of rheumatoid arthritis patients. *J Cell Mol Med*. 2023;27(16):2448–2456.

25. Miao EA, Leaf IA, Treuting PM, et al. Caspase-1-induced pyroptosis is an innate immune effector mechanism against intracellular bacteria. *Nat Immunol*. 2010;11(12):1136–1142.

26. Di A, Kawamura T, Gao XP, et al. A novel function of sphingosine kinase 1 suppression of JNK activity in preventing inflammation and injury. *J Biol Chem*. 2010;285(21):15848–15857.

27. Bai Y, Gomes MT, Prohaska C, Lockett A, Machado RF. Abstract 15143: The Sphk1/S1P/S1PR2 Axis regulates pulmonary vascular remodeling by activating a mitochondrial ROS and NLRP3 inflammasome regulatory loop. *Circulation*. 2022;146:A15143. A15143.

28. Kleinjan A, van Nimwegen M, Leman K, Hoogsteden HC, Lambrecht BN. Topical treatment targeting sphingosine-1-phosphate and sphingosine lyase abrogates experimental allergic rhinitis in a murine model. *Allergy*. 2013;68(2):204–212.

29. Lei YC, Yang LL, Li W, Luo P, Zheng PF. Inhibition of sphingosine kinase 1 ameliorates acute liver failure by reducing high-mobility group box 1 cytoplasmic translocation in liver cells. *World J Gastroenterol*. 2015;21(46):13055–13063.

30. Lin TB, Hsieh MC, Lai CY, et al. Melatonin relieves neuropathic allodynia through spinal MT2-enhanced PP2Ac and downstream HDAC4 shuttling-dependent epigenetic modification of hmgb1 transcription. *J Pineal Res*. 2016;60(3):263–276.

31. Wang J, Cui M, Sun F, et al. HDAC inhibitor sodium butyrate prevents allergic rhinitis and alters lncRNA and mRNA expression profiles in the nasal mucosa of mice. *Int J Mol Med*. 2020;45(4):1150–1162.

32. Nishino TG, Miyazaki M, Hoshino H, Miwa Y, Horinouchi S, Yoshida M. 14-3-3 regulates the nuclear import of class IIa histone deacetylases. *Biochem Biophys Res Commun*. 2008;377(3):852–856.

33. Backs J, Song K, Bezprozvannaya S, Chang S, Olson EN. CaM kinase II selectively signals to histone deacetylase 4 during cardiomyocyte hypertrophy. *J Clin Invest*. 2006;116(7):1853–1864.